ACS FOOD SCIENCE & TECHNOLOGY

pubs.acs.org/acsfoodscitech Article

Glycomic Mapping of the Maize Plant Points to Greater Utilization of the Entire Plant

Garret Couture, Thai-Thanh T. Vo, Juan Jose Castillo, David A. Mills, J. Bruce German, Emanual Maverakis, and Carlito B. Lebrilla*

Cite This: *ACS Food Sci. Technol.* 2021, 1, 2117−2126 Read Online

ACCESS | Metrics & More | Article Recommendations | Supporting Information

ABSTRACT: The goal of food sustainability is possible if greater utilization of plants is achieved. In corn, only the kernels are currently used for human consumption; however, edible carbohydrates that may function as dietary fiber are present throughout the plant. A glycomic map of the maize plant was obtained providing a broad structural view of the carbohydrate distribution revealing that non-cellulosic material was present throughout. Newly developed rapid throughput liquid chromatography tandem mass spectrometry-based methods for analyzing monosaccharide and linkage compositions show unique structural features in the respective segments and parts of the plants from the roots to the tassel. The most abundant monosaccharides of the 14 that were monitored included glucose, xylose, and arabinose. Additionally, galactose, fructose, rhamnose, mannose, galacturonic acid, and glucuronic acid were found in lower abundances. The relative abundances of each monosaccharide varied with the parts of the plants. Linkage compositions also varied and provided further structural information that included the presence of polysaccharides such as xylans, starch, pectins, xyloglucans, arabinans, galactans, and β-glucans. The nonstructural carbohydrate components including the free mono- and disaccharides were also measured to provide a unique geographical map of their abundances. The glycomic map of corn would guide traditional plant breeding methods and new genome editing tools toward tissue-specific enhancements of carbohydrate polymers that have unique and specific functional utility.

KEYWORDS: *plant cell wall, polysaccharides, monosaccharide analysis, linkage analysis, sustainable agriculture, maize*

INTRODUCTION

The world population is estimated to reach nearly 10 billion by the year 2050.[1] Thus, an increased demand on existing food and energy supply chains is expected, especially in the setting of climate change-associated food shortages. Not surprisingly, there is a growing interest in designing multi-purpose crops.[2−6] Carbohydrates, being the most abundant biomolecule class on earth and a component of every food, will play a central role in addressing these issues. In this context, maize constitutes an important opportunity as one of the most widely and abundantly cultivated grains worldwide. Consumption of corn varies by region with the highest among developing countries. Together with wheat, they represent about 80% of cereal requirements in these regions.[7] As food, maize has been bred over millennia to maximize the yield primarily of the grain.[8] There have been enormous resources dedicated to breeding programs that ensure genetic diversity in the collections as well as in the broader global effort to assemble, document, and utilize the resulting efforts. Despite world production reaching 1.1 billion tons in 2020,[7] only a small fraction of that crop is destined for human consumption, the remainder of its dry mass is largely relegated to use as livestock feed and biofuel production.[9] The remaining vegetative tissue after harvest of the grain, the stover, has carbohydrate as its principal component.[10−12] However, current usage of corn stover pays little attention to the potential of this major product as human food. While a large fraction of these carbohydrates is in the form of the linear homopolysaccharide cellulose,[11] there are similarly abundant polysaccharides that are bioactive with functions that include modulating the gut microbiome and can collectively be classified as dietary fiber.[13−16] These carbohydrates could serve as important additional sources of bioenergy and nutrition for animals and humans.

Quantitation of cellulose, the primary component of grass cell walls, requires hydrolysis with sulfuric acid and is readily achieved with well-established protocols.[10,17,18] In contrast, the primary objective in this work was to identify in maize the distributions of more easily fermentable, non-cellulosic polysaccharides, which have potential as alternative sources of human nutrition. The first hurdle to do so was to develop analytic methodologies to detect these non-cellulosic polysaccharides as the existing methods for analysis of diverse cell wall components are outdated, relatively unchanged for decades. These older methodologies involve lengthy sample preparation, long chromatographic run times, and relatively low sensitivity, which impede their use for large sample sets.[17] To address the need for high-throughput analytical methods capable of providing an in-depth structural understanding of

Received: August 31, 2021
Revised: October 20, 2021
Accepted: November 3, 2021
Published: November 24, 2021

https://doi.org/10.1021/acsfoodscitech.1c00318
ACS Food Sci. Technol. 2021, 1, 2117−2126

plant carbohydrates, we developed a robust liquid chromatography tandem mass spectrometry (LC−MS/MS)-based platform for the analysis of plant glycomes. These methods allowed us to quantify the total monosaccharides, free saccharides, and glycosidic linkages within each component of the maize plant. The plant was divided into 213 tissue samples, each subjected to three analyses. The resulting 639 analyses were used to construct an in-depth glycomic map of maize.

Determining carbohydrate components and their spatial distributions throughout the plant in greater detail is the primary focus of this work. These findings provided a much higher resolution picture of corn stover carbohydrate composition than what was previously possible, highlighting more possible nutritional value of this abundant agricultural byproduct. The analytical methodologies developed and employed here are a platform for rapid throughput and robust glycomic mapping of other plants, which will aid in their development as multi-purpose crops and ultimately lead to improved food security. The foundational knowledge and the analytical tools employed could guide selective breeding and genetic modifications to increase the abundances of specific polysaccharides ultimately increasing the crops' sustainability and nutritional and economical value.

EXPERIMENTAL PROCEDURES

Materials. Sodium acetate, trifluoroacetic acid (TFA), chloroform [high-performance liquid chromatography (HPLC) grade], ammonium acetate, ammonium hydroxide solution (NH_4OH) (28−30%), sodium hydroxide pellets (semiconductor grade, 99.99% trace metals basis), dichloromethane, anhydrous dimethyl sulfoxide (DMSO), iodomethane, 3-methyl-1-phenyl-2-pyrazoline-5-one (PMP), methanol (MeOH, HPLC grade), fructose, ribose, rhamnose, mannose, allose, glucuronic acid, galacturonic acid (GalA), glucose, galactose, *N*-acetylglucosamine, *N*-acetylgalactosamine, xylose, arabinose, fucose, maltose, and sucrose were purchased from Sigma-Aldrich (St. Louis, MO). Acetonitrile (HPLC grade) was purchased from Honeywell (Muskegon, MI). Viscozyme was provided by Novozyme (Davis, CA). Nanopure water was used for all experiments.

Preparation of Samples. A 10-foot-tall dent corn plant (*Zea mays* var. *indentata*), also known as field corn, was acquired from a small farm located in Wheatland, California. The plant was harvested 10 weeks after planting and was grown under atmospheric conditions with no additional watering.

The harvested plant was left overnight in the dark before being prepared for sampling. First, the plant was thoroughly washed with nanopure water and staged using a method known within the corn agronomy in the U.S. based on the amount of present leaf collars denoted as discolored line between the leaf blade and leaf sheath with V1 indicating the first leaf closest to the roots and V(n) with (n) being the leaf closest to the tassels.[19] There are two main growth stages, vegetative (V) and reproductive (R) with stage V referring to anatomical parts indirectly related to the corn ear, the R segment. For the convenience of naming, this system was modified to accommodate for the specificity of sample collection. The subject is a V12 plant with 12 leaf collars, dividing the plant into segments called internodes bounded by the nodes above and below. Within each segment, sample collection consisted of a leaf collar, leaf, leaf midrib, stalk sheath, stalk node, and stalk. Each stalk segment was separated into rind and pith (outer and inner, respectively) components when possible. Each component was then further broken down into three or four more parts. For example, the samples "V2 Rind" refer to the outer stalk portions of the segment bounded by the V2 and V3 nodes with the "V2 Rind1" being closest to the V3 node and the "V2 Rind3" sample being closest to the V2 node. The leaves were collected in a similar fashion with "V2 Leaf Tip" being the upper most portion of the leaf blade and the "V2 Leaf Base" being the portion closest to the stalk.

The reproductive stage of this V12 plant has two corn regions denoted as R1 and R2. R1 is the first corn region closest to the roots at V4 segment (V4R1), containing 12 husks with "V4R1 Husk1" being the outermost layer and "V4R1 Husk12" being the innermost layer and closest to the kernels. R2 locates between V5 and V6 and contains 6 husk layers. Each corn region was collected for their kernels, cobs, husks, inner, and outer silk. The corn ear was processed in a similar fashion, as described above, where it was divided into 3−4 equal parts with the kernels carefully separated from their respective cobs.

Other important areas are the tassel and root system. Vt denotes the tassel region with "Vt Stalk" being the stalk where the tassels sprouted, and tassel stems and flowers were collected for analysis. The root system was collected for the nodules and with their nodes, the brace roots and seminal roots above and below the ground level, and the propagating roots.

This highly thorough collection method allowed for a total of 213 samples where each sample was lyophilized to complete dryness before being pulverized into a fine powder using a Bead Ruptor Elite Bead Mill Homogenizer (Omni International, Kennesaw, GA). 10 mg/mL stock solutions of plant tissue were prepared in nanopure water and bullet blended with stainless steel beads at speed four for 2 min before being heated to 100 °C for 1 h. Once cooled, the samples were subjected to one more round of bullet blending.

Free Monosaccharide and Total Monosaccharide Analyses. *Free Saccharide Analysis.* Samples underwent a 10-fold dilution and were transferred to a 96-well plate for derivatization. A cereal quality control sample was also prepared and analyzed alongside the maize samples to assess reproducibility. The coefficients of variation (CVs) for the technical replicates are provided in Table S3b. CVs ranged from less than 1% to about 20%. A procedure using PMP was adapted from Xu et al.[20] Briefly, a pooled standard solution of 14 monosaccharides was prepared and serially diluted to concentrations of 0.001 to 100 μg/mL. Additionally, a standard solution containing the disaccharides sucrose and maltose was prepared and serially diluted to the same concentrations. A solution containing equal parts (v/v) of ammonium hydroxide solution (28−30% v/v) and 0.2 M PMP in methanol was prepared and added to each sample in a 96-well plate. The samples were heated to 70 °C for 30 min followed by vacuum centrifugation to complete dryness. Next, the samples were reconstituted in 250 μL of nanopure water and washed twice with chloroform.

Total Monosaccharide Analysis. Aliquots of each stock solution underwent an enzymatic treatment with Viscozyme (Novozyme, Davis, CA) at 50 °C in 25 mM sodium acetate buffer (pH 5.0). Samples were then subjected to acid hydrolysis with 4 M TFA for 1 h at 121 °C in 96-well plates. Hydrolysis was quenched by the addition of cold nanopure water. The released monosaccharide residues were then derivatized and extracted, according to the procedure previously described. A single sample was chosen and analyzed in triplicate to assess the method reproducibility. The CVs for the technical replicates are provided in Table S1b. In general, CVs of more abundant monosaccharides ranged from about 2 to 11%. Monosaccharides present at low abundance or those more prone to degradation during hydrolysis displayed higher CVs.

Instrumental Analysis. Separation of the PMP-labeled monosaccharides was carried out on an Agilent 1290 Infinity II UHPLC system equipped with a 2-position/10-port switching valve in the column compartment. The LC stack was coupled to an additional binary pump and set up for automated column regeneration. Mass spectral analysis was carried out on an Agilent 6495A triple quadrupole (QqQ) mass spectrometer (Agilent Technologies, Santa Clara, CA). For analysis, 1 μL of the sample was injected onto one of the two Agilent Poroshell HPH C18 column (2.1 mm × 50 mm i.d., 1.8 μm particle size) equipped with Agilent Poroshell HPH C18 guard cartridges (2.1 mm × 5 mm i.d., 1.8 μm particle size). Binary pump 1 was set to a 2.2 min isocratic gradient of 12% B with a constant flow rate of 1.050 mL/min for separation of compounds. Binary pump 2 was set to repeat a column regeneration and equilibration sequence with the following gradient: 0−0.1 min, 12%

https://doi.org/10.1021/acsfoodscitech.1c00318
ACS Food Sci. Technol. 2021, 1, 2117−2126

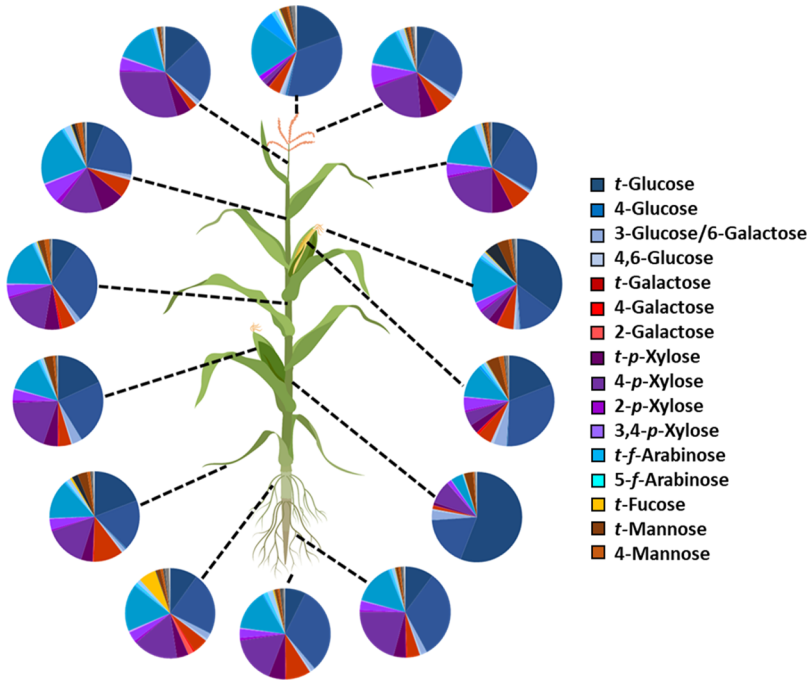

Figure 1. Snapshot of the structural and compositional information obtained by applying rapid throughput, whole-plant glycomic analyses. The pie charts depict the relative glycosidic linkage composition of the indicated tissues. The linkage composition was observed to be highly heterogeneous throughout the plant, indicating that the carbohydrate structures and abundances differed in the various tissues. Created with www.BioRender.com.

B; 0.1−0.2 min, 99% B; 0.2−1.4 min, 99% B; 1.4−1.5 min, 12% B; 1.5−2.2 min, 12% B. Mobile phase A consisted of 25 mM ammonium acetate with pH adjusted to 8.2 with ammonium hydroxide solution in 5% (v/v) acetonitrile. Mobile phase B consisted of 95% (v/v) acetonitrile in water.

Linkage Analysis. *Permethylation, Hydrolysis, and Derivatization of Plant Tissue Samples.* A permethylation procedure was adapted from Galermo et al.[21,22] Aliquots containing 50 μg of plant tissue were transferred to a 96-well plate and permethylated using iodomethane in a solution of DMSO containing saturated NaOH. The samples were allowed to react on a shaker at room temperature for 50 min under argon before being quenched by the addition of cold water. A liquid−liquid extraction using dichloromethane and cold water was performed and repeated five times to remove excess NaOH and DMSO. The upper aqueous layer was discarded, while the bottom organic layer containing permethylated products was dried to completion by vacuum centrifugation. Permethylated samples were then subjected to acid hydrolysis at 100 °C with 4 M TFA and subsequently dried by vacuum centrifugation. The released permethylated monosaccharide residues were derivatized with PMP following the previously described procedure. A single sample was chosen and analyzed in triplicate to assess the method reproducibility. The CVs for the technical replicates are provided in Table S2b. Abundant linkage CVs ranged from about 7 to 20%, while those present at trace levels tended to display higher CVs.

Instrumental Analysis. Separation and analysis of the permethylated glycosides were carried out on an Agilent 1290 Infinity II UHPLC system coupled to an Agilent 6495A triple quadrupole (QqQ) mass spectrometer (Agilent Technologies, Santa Clara, CA). For analysis, 1 μL of the sample was injected onto an Agilent Zorbax RRHD Eclipse Plus C18 column (2.1 mm × 150 mm i.d., 1.8 μm particle size) equipped with an Agilent Zorbax Eclipse Plus C18 guard cartridge (2.1 mm × 5 mm i.d., 1.8 μm particle size) and separated using a 15 min binary gradient with a constant flow rate of 0.22 mL/min. Mobile phase A consisted of 25 mM ammonium acetate with pH adjusted to 8.2 with ammonium hydroxide solution in 5% (v/v) acetonitrile. Mobile phase B consisted of 95% (v/v) acetonitrile in water. The following binary gradient was used: 0.00−5.00 min, 21.00% B; 5.00−9.00 min, 21.00−22.00% B; 9.00−11.00 min, 22.00% B; 11.00−13.60 min, 22.00−24.50% B; 13.60−13.61 min, 24.50−99.00% B; 13.61−13.80 min, 99.00% B; 13.80−13.81 min, 99.00−21.00% B; 13.81−15.00 min, 21.00% B. Samples were introduced into the mass spectrometer using an electrospray ionization source operated in the positive ion mode. Nitrogen drying and sheath gas temperatures were set at 290 and 300 °C, respectively. Drying and sheath gas flow rates were set at 11 and 12 L/min, respectively. The nebulizer pressure was set to 30 psi. Capillary and fragmentor voltages were set at 1800 and 380 V, respectively. Data were acquired using the multiple reaction monitoring (MRM) mode. The collision energy was set to 35 eV. Data analysis was performed using Agilent MassHunter Quantitative Analysis software version B.08.00.

RESULTS AND DISCUSSION

Overview of Analytical Workflow. A rapid throughput, LC−MS-based workflow was developed and employed for the profiling of both structural and non-structural carbohydrates in plant tissues. A snapshot highlighting the utility of the methodology is provided in Figure 1. This workflow consisted of three separate analyses each applied to all 213 tissue samples, providing unique information toward the overall carbohydrate composition of the maize plant. Total monosaccharide compositional analysis was performed first. This analysis provided quantitative information on the total non-cellulosic carbohydrates present. Glycosidic linkage compositional analysis was then performed to determine how the observed monosaccharide residues were connected and provide structural information. The monosaccharide and linkage compositions provided general information on the polysaccharide compositions throughout the maize plant. Lastly, free saccharide analysis was performed to understand how non-structural carbohydrates such as free fructose, glucose, and sucrose were distributed throughout the tissues of the plant.

Monosaccharide Composition Map of the Maize Plant. To obtain quantitative information on the non-

https://doi.org/10.1021/acsfoodscitech.1c00318
ACS Food Sci. Technol. 2021, 1, 2117−2126

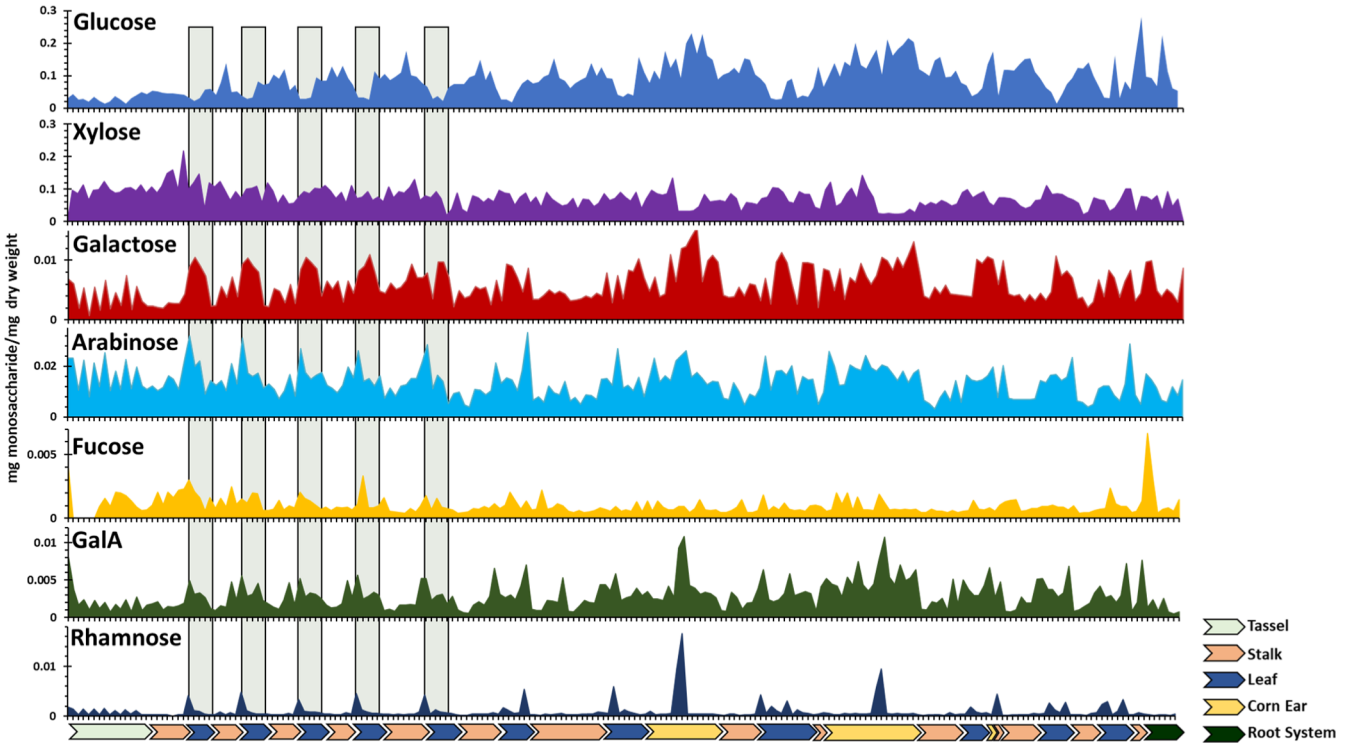

Figure 2. Total monosaccharide composition of the maize plant from top to bottom (left to right). The most abundant monosaccharides detected are shown (note the different scales of the axes). The colored bar along the *x*-axis and key indicate the tissue type. Monosaccharide compositions differed between tissues with the stalk containing more glucose than other portions of the plant. The leaves consistently displayed more galactose, arabinose, and GalA than the stalk especially toward the top of the plant (highlighted with shaded green boxes). The leaf collars are readily identified by their large rhamnose content, while the brace roots their fucose content.

cellulosic structural carbohydrates, we subjected each tissue sample to the optimized workflow for absolute quantitation of monosaccharides. Figure S1 shows the extracted ion chromatograms (EICs) of all monosaccharides contained in the standard pool that were quantified in the maize plant. The respective retention times, MRM transitions, and collision energies are detailed in Table S4. Of the 14 monosaccharides monitored in the method, glucose, xylose, and arabinose were the most abundant throughout the plant. Galactose, fructose, rhamnose, mannose, GalA, glucuronic acid, and fucose were also present with lower abundances (Figure 2, Table S1a).

Large differences in the total monosaccharide composition were observed across different tissues. The leaves showed relatively small amounts of glucose relative to the stalk, while galactose, arabinose, and GalA were found to be significantly higher in abundances. The tassels also exhibited increased abundances of these monosaccharide residues relative to the stalk and roots. Galactose, arabinose, and GalA are constituents of pectins, suggesting that the pectin content of the leaves and tassels was significantly higher than that in the stalk. Similarly, the abundances of GalA were significantly higher in the stalk pith relative to the stalk rind throughout the plant (Figure S2). The average GalA content was also found to be highest collectively in the corn ears, lesser in the leaves, and even less in the stalk (Figure S3). Because GalA belongs principally to pectic polysaccharides, the results likely indicate higher pectin content in the corn ears. The leaf collars contained a significantly greater abundances of rhamnose compared to all other stalk tissues. The brace roots contained significantly more fucose than all other tissues. Coincidently, secretions of aerial roots in a landrace maize from Sierra Mixe contain similarly high levels of fucose, which is commonly found in animal carbohydrates and more unusual in plants.[23] The corn husks, like the leaves, contained greater amounts of glucose, galactose, arabinose, and GalA compared to other tissues. The corn kernels and cobs, however, had the highest total glucose abundances and lowest non-glucose residues, owing to their relatively high starch content (Figure 2).

Plotting the monosaccharide abundances between different monosaccharides yielded correlations pointing to specific polysaccharides (Figure 3). The combination of galactose, arabinose, and GalA, when correlated point to the presence of pectin. Along the stalk, xylose and arabinose produced strong positive correlations, and both tended to increase toward the top of the plant (Figure 3). The two monosaccharides make up arabinoxylans, which are constituent polysaccharides of several foods including rice and other grains.[12,24,25] Xylose and arabinose were negatively correlated with glucose (primarily from starch), suggesting that the presence of starch corresponds to the absence of arabinoxylans. Starch was therefore greater at the bottom of the plant, and arabinoxylans were greater toward the top of the plant.

Glycosidic Linkage Distribution in Maize. The structural characteristics and relative abundances of the polysaccharides present in each sample were determined using glycosidic linkage analysis. Linkage analysis was performed using a recently developed rapid throughput method that yielded relative quantitation.[21,22] Figure S4 shows the EICs of each linkage represented in a pool of oligosaccharide standards containing the most common linkages encountered in plants. Retention times, MRM transitions, and collision energies are provided in Table S5.

https://doi.org/10.1021/acsfoodscitech.1c00318
ACS Food Sci. Technol. 2021, 1, 2117−2126

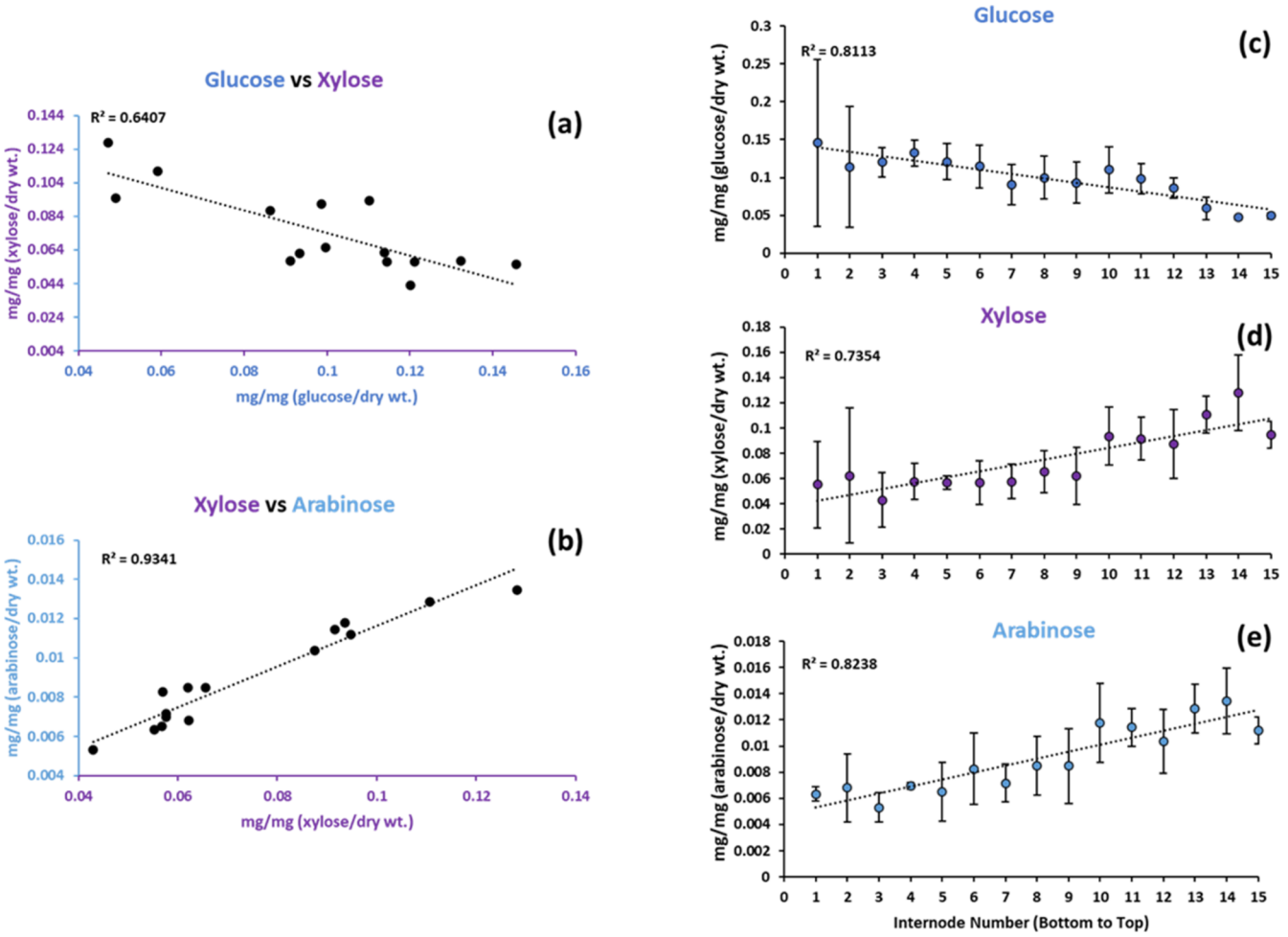

Figure 3. Relationship between the three most abundant monosaccharides (glucose, xylose, and arabinose) detected in maize stalk. Each point represents an internode for which all tissue samples in that internode were averaged. (a) Glucose and xylose displayed a strong negative correlation throughout the stalk. (b) Xylose and arabinose displayed a strong positive correlation throughout the stalk. (c) Concentration of glucose in maize internodes decreased from top to bottom of the plant. (d) Xylose and (e) arabinose concentration decreased in internodes from top to bottom of the plant. Error bars represent the standard deviation.

Linkage analysis confirmed trends observed in the monosaccharide analysis and provided specific information on the structural features of the polysaccharides present in each tissue. The method monitors nearly 100 different linkages; however, only 34 were observed in the sample. Based on this analysis, 4-linked glucose (4-Glc), 4-linked xylose (4-Xyl), and terminal arabinose (*t*-Ara) comprised the largest fraction (Figure 4, Table S2a), indicating that the majority of the carbohydrate content throughout the plant comprised cellulose and xylans. Due to the nature of the methods, linkage analysis samples the cellulose, while monosaccharide analysis does not. The two branching residues, 2,4- and 3,4-xylose, together with a large abundance of *t*-Ara also indicated the presence of arabinoxylan throughout the plant.[17] This arabinoxylan structure could be further described as being branched primarily through a 3,4-xylose linkage, which was the primary branching residue detected in analysis.

The next most abundant linkages were terminal xylose and terminal galactose, which were accompanied by increases in 2-xylose (Figure S5). Together, this provided evidence that xyloglucan was the most abundant hemicellulose present after xylans, which was consistent with what was known of grass cell walls.[26,27] Furthermore, these xyloglucan-associated linkages were found to be higher in the tassel flower, leaf, husk, and root tissues compared to the stalk.

Linkage analysis also revealed structural information and relative abundances of the more minor hemicellulose components present in differing amounts throughout the plant. Terminal-, 4-, and 4,6-mannose residues were detected in all tissue samples, indicating that the cell walls contained small amounts of mannans (Figure S6). These residues had higher abundances specifically in the stalk nodes and leaf collars. The stalk regions below the corn ears also tended to have higher amounts of these linkages than the same tissues above. In addition to mannan-associated linkages, 3-linked glucose was also detected throughout the plant, indicating the possible presence of β-glucan (Figure S7). Overall, this linkage generally displayed the lowest abundances in the leaf blades, tassels, and roots with the highest abundances in the stalk nodes, stalk sheaths, and corn husks followed by the leaf midribs and stalk tissues. Below the ears of corn, the stalk tended to contain more of the 3-linked residue relative to stalk tissues mentioned above.

The increased arabinose content seen in the total monosaccharide analysis of the leaves were found to be due to relative increases in 2- and 3-arabinose, suggesting a

https://doi.org/10.1021/acsfoodscitech.1c00318
ACS Food Sci. Technol. 2021, 1, 2117−2126

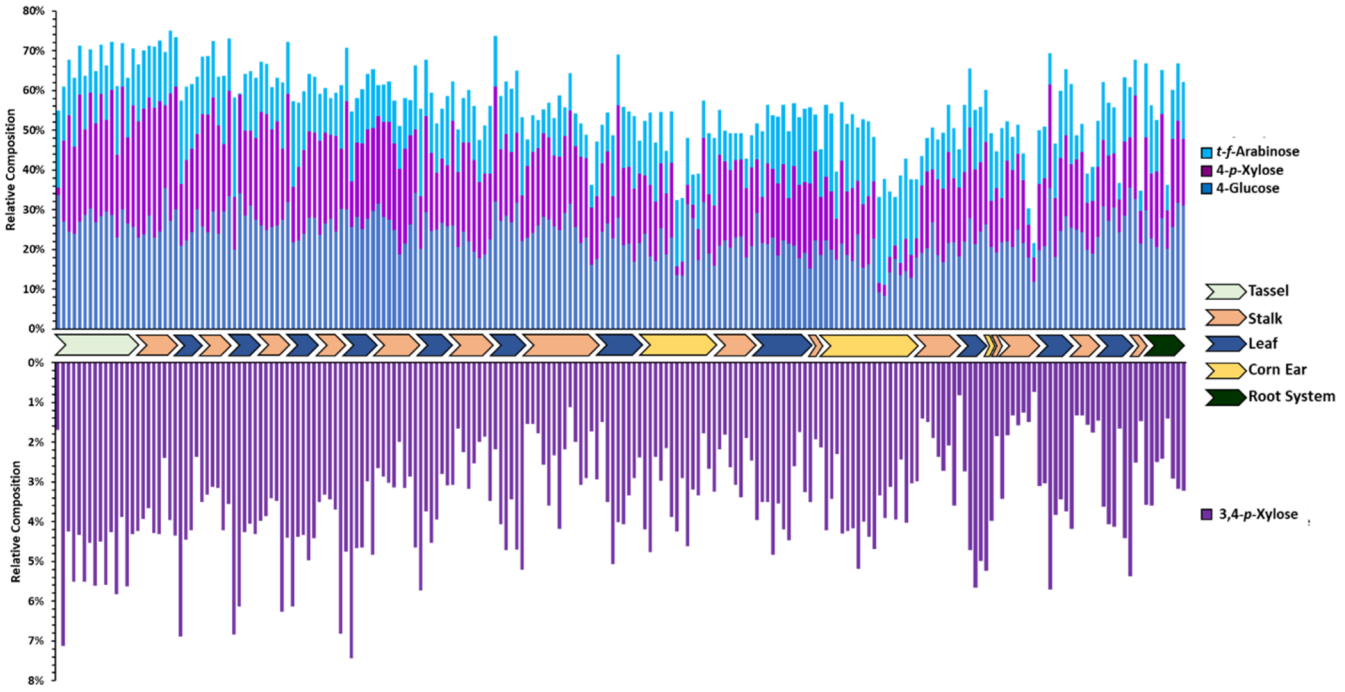

Figure 4. Most abundant glycosidic linkages detected throughout the maize plant. The large amounts of 4-glucose, 4-xylose, 3,4-xylose, and *t*-arabinose indicated that cellulose, xylan, and arabinoxylan were the most abundant polysaccharides present throughout the plant. However, their distributions were heterogeneous with the lower portions of the stalk containing less branching residues.

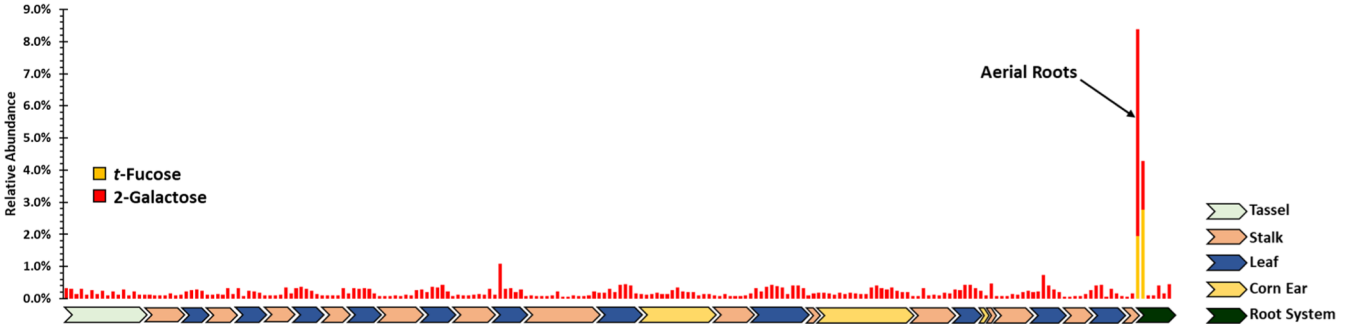

Figure 5. Brace roots and node displayed the highest abundance of *t*-fucose, while 2-galactose was exclusively observed in these tissues. These linkages likely belong to a selectively fucosylated xyloglucan or mucilage polysaccharide structure.

corresponding increase in branched arabinans (Figure S8).[28,29] On the other hand, the absolute galactose content of the leaves was noted to correspond to similar increases in 4-, 6-, 3,6-linked and terminal galactose residues. The increases in 4-galactose, however, seemed to be associated only with the stalk node and stalk sheath (Figure S9), while the 6- and 3,6-galactose were noted to be associated with the leaves themselves (Figure S10). This finding suggested differences in the side-chain structures of the pectic polysaccharides within these tissues. The 4-galactose indicated linear galactan, while the 6- and 3,6-linkages are unique to arabinogalactan.[17]

Unique compositional differences were observed in the brace roots and pollen of the maize plant. The brace roots displayed the highest concentration of fucose compared to all other plant tissues, and this finding was confirmed by linkage analysis, which produced terminal fucose (*t*-Fuc). Furthermore, 2-galactose was observed only in these tissues (Figure 5). These observations together suggested the presence of a uniquely fucosylated polysaccharide such as a fucosylated xyloglucan or the remnants of a mucilage containing both *t*-Fuc and 2-Gal that was previously found in a landrace of maize from Sierra Mixe.[23,30]

The pollen had very little xylose and instead contained elevated amounts of galactose, fucose, rhamnose, GalA, and arabinose. Despite the sample size, the analytical platform was sufficiently sensitive to elucidate the structures of even small plant components. Linkage analysis revealed relatively higher abundances of 6-galactose, *t*-galactose, *t*-fucose, 5-arabinose, 3-arabinose, and 2-arabinose with 2,5-arabinose being detected exclusively in the pollen. The total monosaccharide and linkage analysis of the pollen suggests the presence of a cell wall rich in pectic polysaccharides.[28,29]

Free Mono- and Disaccharide Distribution in the Maize Plant. The distribution of free mono- and disaccharides were quantitatively measured throughout the whole plant. Of the 16 compounds (monosaccharides and two disaccharides) monitored, glucose, fructose, and sucrose were found to be the most abundant free mono- and disaccharides (Table S3a). The concentration of each was markedly different both across and within tissues (Figure 6). Total free sugar

https://doi.org/10.1021/acsfoodscitech.1c00318
ACS Food Sci. Technol. 2021, 1, 2117−2126

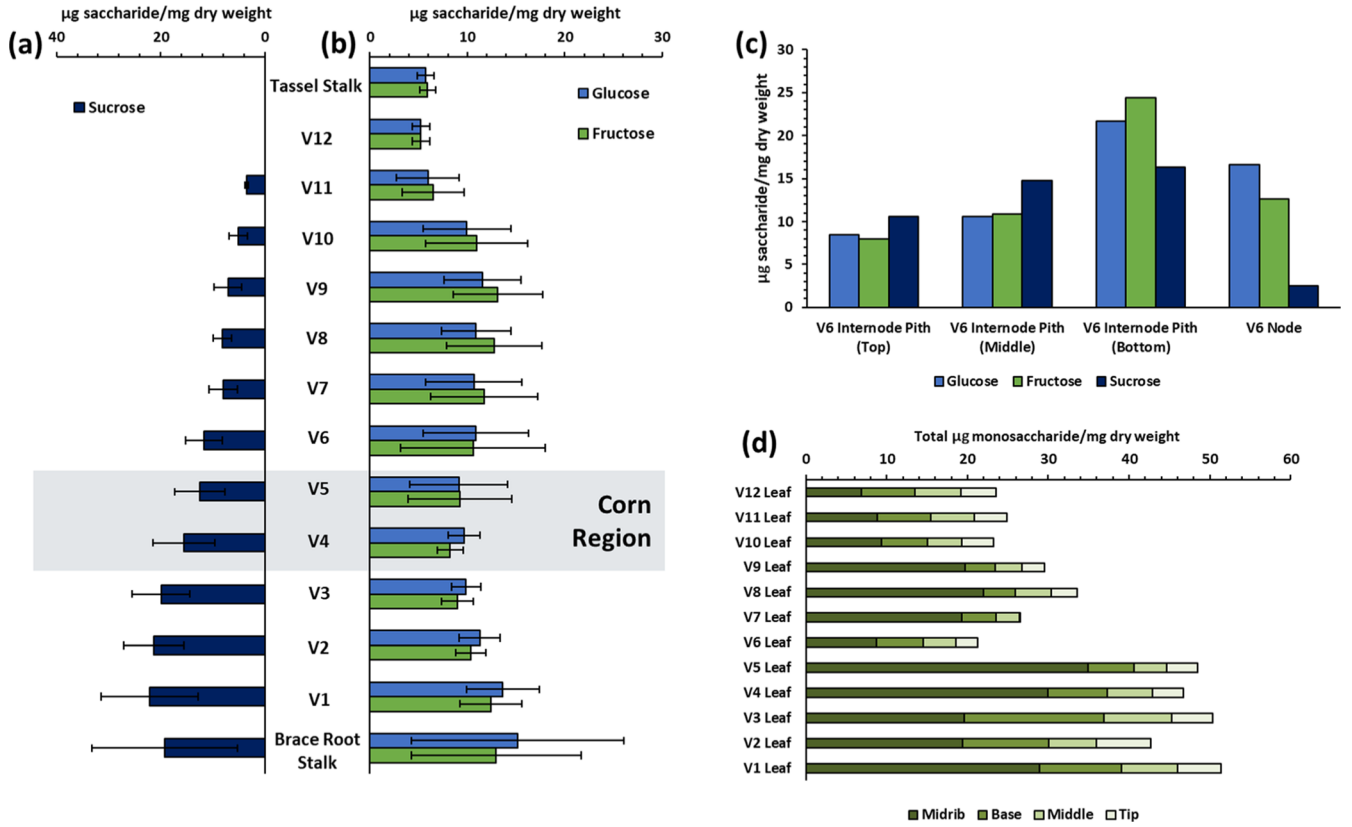

Figure 6. Distribution of free glucose, fructose, and sucrose in the stalk and leaf tissues. (a,b) Concentration of sucrose and glucose/fructose, respectively, in all stalk internodes from top to bottom of the plant. Bars indicate averages of all samples taken within each internode. Error bars represent the standard deviation. (c) Example of heterogeneous distribution of free sugars within internodes. The pith just above the node tended to contain the most sugars, while the nodes were consistently low or void of sucrose. (d) Sum of fructose and glucose concentrations in each sample within each leaf. Sugar concentrations were observed to follow an increasing gradient from leaf tip to middle, base, and midrib. Leaves below the corn ears (V5−V1) contained significantly more free sugars than those above the corn ears (Student's *t*-test, $p < 3 \times 10^{-6}$).

(fructose, glucose, and sucrose) concentrations increased from the top to bottom of the plant. However, sucrose was found to be sequestered in the stalk, while the highest concentrations of glucose and fructose were found in the tissues of the corn ears. Furthermore, leaves were observed to contain minimal mono- and disaccharides with the majority being found in the stalk.

In addition to differences between tissues, there were also variations within tissues. The average concentration of free sugars increased from the top to bottom of the stalk (Figure 6a). Furthermore, the free sugar concentration tended to increase from top to bottom in the pith of each internode. The stalk nodes, however, were consistently low or void of sucrose (Figure 6c). The leaves showed a similar trend where the sugar concentrations tended to follow a gradient from the tip of each leaf to its base, while the midribs consistently contained the highest concentrations (Figure 6d). In addition, the leaves below the corn ears contained significantly higher free sugar concentrations than those found above.

Full Glycomic View of the Maize Plant. Carbohydrates as human food provide energy and growth due to the presence of glucose, primarily as starch, free glucose, fructose, and sucrose. A map of glycans and polysaccharides in plants can provide parts of the plants that can be consumed and used particularly as fiber. Human digestive enzymes are limited to cleaving polysaccharides with α(1,4)-glucose bonds. Polysaccharides in food that are not cleaved by the host enzymes are called fiber, a broad general term with little structural specificity. The utility to digest fiber is obtained by recruiting microbes with a wide array of carbohydrate-active enzymes (CAZymes) that can cleave a wide range of glycosidic linkages including those from cellulose.[13] CAZymes such as glycosyl hydrolases (GHs) and polysaccharide lyases (PLs) in the microbiome are highly selective and limited to specific linkages. For example, the major glycosidic linkages 4-Glc, 4-Xyl, and *t-f*-Ara from cellulose and (arabino)xylan observed here could be cleaved by any number of microbial β-glucanases, β-xylanases, and α-arabinosidases, respectively. Although there has been considerable effort in characterizing the microbiome and its role in health and nutrition, much less is known regarding the structures of the food that modulate the microbiome. However, the key to understanding the microbiome and in developing better synbiotics (the combination of pre- and probiotic) lies in knowing the structures of food and the specificity of the bacterial enzymes. The cell wall polysaccharide components of maize can thus be used to target specific enzymatic functionalities in the gut microbiome with the goal of altering the composition of the bacterial community and host health. This concept has been demonstrated in pea and orange fiber preparations, in which supplementation caused increases in the expression of GHs and PLs specific to the polysaccharides comprising the fibers.[31] Likewise, maize fiber preparations with their primary constituents being cellulose, (arabino)xylan, and xyloglucan could be used for target gut microbial species possessing β-glucanases (4-Glc), β-xylanases (4-Xyl), and α-arabinofuranosidases (*t-f*-Ara). Common plant breeding practices will soon

https://doi.org/10.1021/acsfoodscitech.1c00318
ACS Food Sci. Technol. 2021, 1, 2117−2126

be supplemented by gene-editing tools like CRISPR to provide powerful tools to answer global food supply, agricultural, and bioenergy demands.[6,32] While the focus of these efforts have been on the grain, modern agriculture should instead broaden it to produce a more broadly useable plant. However, the lack of structural targets in various tissues constrained the utility of these methods. Previous investigations of the maize carbohydrate composition have characterized a limited number of polysaccharides from a relatively small number of tissues in the plant.[10,33−35] These earlier approaches lacked the sensitivity, quantitation, and sample throughput to provide the spatial distributions of the diverse structural and non-structural carbohydrates in crops. However, such information will help interpret the outcomes of gene-editing and breeding experiments at the whole organism level, accelerating the development of defined multi-purpose crops.

The carbohydrate map can also elucidate the fundamental mechanism of carbohydrate storage and function in plants. The cellulose microfibrils in grass cell walls are thought to be cross-linked and non-covalently bound by xylan and glucuronoxylan through hydrogen bonding interactions. This association is thought to add structural rigidity to the cell wall.[36,37] Substitution of xylan with arabinosyl residues as in arabinoxylan decreases the extent to which hydrogen bonding can occur, resulting in less cell wall rigidity. Thus, it is thought that grass cell elongation is positively correlated to xylan substitution with arabinose.[38] These conclusions are consistent with observations here. Both total xylose and 4-xylose abundance were consistent in leaf tissues. In the stalk, however, segments toward the top of the plant tended to display greater total and 4-xylose content than segments toward the bottom of the plant. In addition, the top segments of the stalk displayed greater amounts of 3,4-xylose and terminal arabinose indicative of a greater arabinoxylan content. The general decrease in the xylan content toward the more mature, bottom portions of the stalk may also suggest that wall hardening in those tissues is due to other processes such as lignification rather than xylan cross-linking.[25] Lignification is a prevalent feature of the maize cell wall known to increase recalcitrance and decrease digestibility.[2] The analytical methodology employed here does not capture this feature; however, lignin can be measured using several well-established protocols.[39] The leaves also tended to have a greater abundance of 3,4-xylose relative to the stalk, indicating a greater degree of arabinose branching. If these hypotheses are true, the more branched xylan structures in the top portions of the plant and leaves could be more easily extracted or digested due to their weaker association with the cellulose framework, thus also resulting in less cellulosic recalcitrance.[2] This could make certain portions of harvested plants more attractive and more efficient sources for a variety of uses including feed and biofuel production.

Although a minor hemicellulose component in grass cell walls,[24] xyloglucan may play a role in cell elongation, morphogenesis, and as a component of root mucilage.[30,36,40] We identified xyloglucan here by the *t*-Gal, *t*-Xyl, and 2-Xyl linkage, although *t*-Gal may also be present in pectic sidechains.[17] In grasses, substitutions are most commonly observed not to extend past the *t*-Xyl residue.[41] However, structures exhibiting galactose have been reported, and occurrence can even be tissue-dependent.[42] Indeed, the 2-Xyl linkage was detected throughout the plant here and found to be less abundant in the stalk relative to leaf, husk, and root tissues. Most notably, each leaf collar exhibited significantly higher 2-Xyl levels than surrounding tissues. The abundance of these xyloglucan-associated linkages as a whole was found to be increased in the leaf tissues and tended to decrease from top to bottom portions of the stalk. This finding supports more recent evidence that xyloglucan comprises a larger fraction of the cell wall in meristematic cells, likely present in the more immature tissues of the upper stalk and may play an important role in cell elongation and morphogenesis.[24,36,40,43] Furthermore, these findings suggest that xyloglucan structure may dictate different physiological functions that are yet to be fully resolved. The xyloglucan-associated linkages were also found to increase in the propagating roots, supporting its putative role as a mucilage secreted into the rhizosphere.[30]

The presence of β-glucan in the cell wall is a feature quite unique to grasses. Its presence in grain has been proposed as an alternate storage polysaccharide during certain development stages and under some environmental conditions.[44,45] Early studies into its function in the cell wall also found its accumulation in the elongation phase of coleoptiles, leading to the conclusion that β-glucan plays a role in this process.[24] However, more recent studies have also shown accumulation of β-glucan in mature stalk tissues of several grass species including maize suggesting a more complex role than previously thought.[46] The relative abundance of 3-glucose was used as a proxy to compare the β-glucan content throughout the maize plant in the present study. An observation unique to this whole-plant glycomic view is the distribution of this 3-linked glucose residue follows the distribution of free glucose, free fructose, and sucrose throughout the plant. This supports the notion that β-glucan functions as an alternate storage polysaccharide not only in the developing corn kernels of the primary sink but also in the mature stalk tissues of the secondary sink.

Grass cell walls are known to contain relatively little pectin, but this component nonetheless plays many important roles in the primary cell wall, including wall strength, cell adhesion, and cell defense.[47] Pectins are the most structurally diverse group of cell wall polysaccharides and can be comprising polygalacturonan and rhamnogalacturonan I/II in addition to extensive neutral sidechains such as arabinan, galactan, and arabinogalactan.[28,29,47] Elucidation of these structures when isolated is a challenging task and analyzing whole tissue as done here only adds to the complexity. However, pectins contain several distinctive structural features that can provide information on how the pectin content and structure change throughout the plant. The pectin backbone can be comprising exclusively GalA as in polygalacturonan or include rhamnose as in rhamnogalacturonan.[28,29,47] Because these monosaccharide residues belong principally to pectins, they were used to describe the overall pectin content and rhamnogalacturonan content between tissues. GalA was generally found in greater abundance in the pollen, flowers, leaves, and corn ears relative to the tissues of the stalk and root. Furthermore, the inner stalk was found to have more GalA than the outer stalk throughout its length. However, the most significant GalA content was observed in the pollen, stalk nodes, leaf collars, and silk, indicating the highest pectin content in these tissues. Distribution of rhamnose followed a more pronounced trend with definitive spikes at the leaf collars, perhaps indicating particularly large amounts of rhamnogalacturonan in these tissues. Furthermore, the rhamnose content followed a gradient in each leaf blade with the highest concentration

https://doi.org/10.1021/acsfoodscitech.1c00318
ACS Food Sci. Technol. 2021, 1, 2117−2126

observed in the base and the lowest at the tip of the leaf. A large fraction of the rhamnose residues in rhamnogalacturonan are substituted with neutral side chains like arabinan, galactan, and arabinogalactan. The presence of these structures is thought to add flexibility to the cell wall by preventing the formation of cellulose microfibrils.[36] Here, the arabinan-associated linkages 2-, 3-, and 5-arabinose were found to have increased abundance in all leaf tissues and tassel flowers. Arabinogalactan-associated linkages 6- and 3,6-galactose were also found to have increased abundance. This finding, along with the greater abundance of the branching 3,4-xylose linkage in xylan, may provide a polysaccharide-based rationale for the decreased recalcitrance and increased flexibility of leaf tissues relative to the stalk. Together, these findings successfully illustrate a comprehensive map of the carbohydrates present in the maize plant. The methods employed to generate this map are rapid throughput, adaptable, and can be utilized to elucidate functional features of carbohydrates in plants. The results of these experiments will provide a unique perspective toward genetic traits of the entire corn plant in particular, but in principle all agricultural food candidates make for better human and animal nourishment, crop efficiency, soil regeneration, and agricultural sustainability.

■ ASSOCIATED CONTENT

Supporting Information

The Supporting Information is available free of charge at https://pubs.acs.org/doi/10.1021/acsfoodscitech.1c00318.

Heterogeneous distribution of monosaccharide and glycosidic linkage residues observed throughout the maize plant (PDF)

Total monosaccharide composition of the maize plant; monosaccharide composition and CV of technical replicates; glycosidic linkage composition of the maize plant; glycosidic linkage composition and CV of technical replicates; free mono- and disaccharide content of the maize plant; free mono- and disaccharide content and CV of technical replicates; monosaccharide analysis retention times, MRM transitions, and collision energies; and linkage analysis retention times, MRM transitions, and collision energies (XLSX)

■ AUTHOR INFORMATION

Corresponding Author

Carlito B. Lebrilla − *Department of Chemistry, University of California Davis, Davis, California 95616, United States; Foods for Health Institute and Department of Biochemistry and Molecular Medicine, University of California Davis, Davis, California 95616, United States;* orcid.org/0000-0001-7190-5323; Phone: +1 530 752 6364; Email: cblebrilla@ucdavis.edu; Fax: +1 530 752 8995

Authors

Garret Couture − *Department of Chemistry, University of California Davis, Davis, California 95616, United States; Foods for Health Institute, University of California Davis, Davis, California 95616, United States;* orcid.org/0000-0002-8947-4354

Thai-Thanh T. Vo − *Department of Chemistry, University of California Davis, Davis, California 95616, United States; Foods for Health Institute, University of California Davis, Davis, California 95616, United States*

Juan Jose Castillo − *Department of Chemistry, University of California Davis, Davis, California 95616, United States; Foods for Health Institute, University of California Davis, Davis, California 95616, United States;* orcid.org/0000-0001-9680-5273

David A. Mills − *Department of Food Science and Technology, University of California Davis, Davis 95616 California, United States*

J. Bruce German − *Department of Food Science and Technology, University of California Davis, Davis 95616 California, United States*

Emanual Maverakis − *Department of Dermatology, School of Medicine and Institute for Regenerative Cures, University of California Davis, Sacramento, California 95817, United States*

Complete contact information is available at: https://pubs.acs.org/10.1021/acsfoodscitech.1c00318

Author Contributions

G.C. and T.-T.T.V. performed all experiments, analysis of samples, produced all figures and tables, and wrote the manuscript. J.J.C. aided in experimental planning and edited the manuscript. D.A.M., J.B.G, and E.M. aided in editing the manuscript. C.B.L. planned the overall experimental project and reviewed the manuscript.

Notes

The authors declare no competing financial interest.

■ REFERENCES

(1) *World Population Prospects 2019: Highlights*; United Nations, Department of Economic and Social Affairs, Population Division, 2019.

(2) Himmel, M. E.; Ding, S.-Y.; Johnson, D. K.; Adney, W. S.; Nimlos, M. R.; Brady, J. W.; Foust, T. D. Biomass recalcitrance: engineering plants and enzymes for biofuels production. *Science* **2007**, *315*, 804−807.

(3) Ragauskas, A. J.; Williams, C. K.; Davison, B. H.; Britovsek, G.; Cairney, J.; Eckert, C. A.; Frederick, W. J., Jr.; Hallett, J. P.; Leak, D. J.; Liotta, C. L.; Mielenz, J. R.; Murphy, R.; Templer, R.; Tschaplinski, T. The path forward for biofuels and biomaterials. *Science* **2006**, *311*, 484−489.

(4) Loqué, D.; Scheller, H. V.; Pauly, M. Engineering of plant cell walls for enhanced biofuel production. *Curr. Opin. Plant Biol.* **2015**, *25*, 151−161.

(5) Slewinski, T. L. Non-structural carbohydrate partitioning in grass stems: a target to increase yield stability, stress tolerance, and biofuel production. *J. Exp. Bot.* **2012**, *63*, 4647−4670.

(6) Khan, M. Z.; Zaidi, S. S.-E.-A.; Amin, I.; Mansoor, S. A CRISPR Way for Fast-Forward Crop Domestication. *Trends Plant Sci.* **2019**, *24*, 293−296.

(7) *Grain: World Markets and Trade*; United States Department of Agriculture, 2021.

(8) Yang, C. J.; Samayoa, L. F.; Bradbury, P. J.; Olukolu, B. A.; Xue, W.; York, A. M.; Tuholski, M. R.; Wang, W.; Daskalska, L. L.; Neumeyer, M. A.; Sanchez-Gonzalez, J. d. J.; Romay, M. C.; Glaubitz, J. C.; Sun, Q.; Buckler, E. S.; Holland, J. B.; Doebley, J. F. The genetic architecture of teosinte catalyzed and constrained maize domestication. *Proc. Natl. Acad. Sci. U.S.A.* **2019**, *116*, 5643−5652.

(9) McConnell, M.; Liefert, O.; Capehart, T.; Ramsey, S. *Feed Outlook*; USDA ERS, 2021.

(10) Santoro, N.; Cantu, S. L.; Tornqvist, C.-E.; Falbel, T. G.; Bolivar, J. L.; Patterson, S. E.; Pauly, M.; Walton, J. D. A High-Throughput Platform for Screening Milligram Quantities of Plant Biomass for Lignocellulose Digestibility. *Bioenerg. Res.* **2010**, *3*, 93−102.

(11) Penning, B. W.; Shiga, T. M.; Klimek, J. F.; SanMiguel, P. J.; Shreve, J.; Thimmapuram, J.; Sykes, R. W.; Davis, M. F.; McCann, M. C.; Carpita, N. C. Expression profiles of cell-wall related genes vary broadly between two common maize inbreds during stem development. *BMC Genomics* **2019**, *20*, 785.
(12) Hatfield, R. D. Structural Polysaccharides in Forages and Their Degradability. *Agron J.* **1989**, *81*, 39−46.
(13) Martens, E. C.; Kelly, A. G.; Tauzin, A. S.; Brumer, H. The Devil Lies in the Details: How Variations in Polysaccharide Fine-Structure Impact the Physiology and Evolution of Gut Microbes. *J. Mol. Biol.* **2014**, *426*, 3851−3865.
(14) Sonnenburg, E. D.; Sonnenburg, J. L. Starving our Microbial Self: The Deleterious Consequences of a Diet Deficient in Microbiota-Accessible Carbohydrates. *Cell Metab.* **2014**, *20*, 779−786.
(15) Flint, H. J.; Scott, K. P.; Duncan, S. H.; Louis, P.; Forano, E. Microbial degradation of complex carbohydrates in the gut. *Gut Microbes* **2012**, *3*, 289−306.
(16) Flint, H. J.; Bayer, E. A.; Rincon, M. T.; Lamed, R.; White, B. A. Polysaccharide utilization by gut bacteria: potential for new insights from genomic analysis. *Nat. Rev. Microbiol.* **2008**, *6*, 121−131.
(17) Pettolino, F. A.; Walsh, C.; Fincher, G. B.; Bacic, A. Determining the polysaccharide composition of plant cell walls. *Nat. Protoc.* **2012**, *7*, 1590−1607.
(18) Rongpipi, S.; Ye, D.; Gomez, E. D.; Gomez, E. W. Progress and Opportunities in the Characterization of Cellulose - An Important Regulator of Cell Wall Growth and Mechanics. *Front Plant Sci.* **2018**, *9*, 1894.
(19) Abendroth, L.; Elmore, R. W.; Boyer, M. J.; Marlay, S. K. *Corn Growth and Development*; Kansas State University, 2011.
(20) Xu, G.; Amicucci, M. J.; Cheng, Z.; Galermo, A. G.; Lebrilla, C. B. Revisiting monosaccharide analysis - quantitation of a comprehensive set of monosaccharides using dynamic multiple reaction monitoring. *Analyst* **2017**, *143*, 200−207.
(21) Galermo, A. G.; Nandita, E.; Barboza, M.; Amicucci, M. J.; Vo, T.-T. T.; Lebrilla, C. B. Liquid Chromatography-Tandem Mass Spectrometry Approach for Determining Glycosidic Linkages. *Anal. Chem.* **2018**, *90*, 13073−13080.
(22) Galermo, A. G.; Nandita, E.; Castillo, J. J.; Amicucci, M. J.; Lebrilla, C. B. Development of an Extensive Linkage Library for Characterization of Carbohydrates. *Anal. Chem.* **2019**, *91*, 13022−13031.
(23) Amicucci, M. J.; Galermo, A. G.; Guerrero, A.; Treves, G.; Nandita, E.; Kailemia, M. J.; Higdon, S. M.; Pozzo, T.; Labavitch, J. M.; Bennett, A. B.; Lebrilla, C. B. Strategy for Structural Elucidation of Polysaccharides: Elucidation of a Maize Mucilage that Harbors Diazotrophic Bacteria. *Anal. Chem.* **2019**, *91*, 7254−7265.
(24) Carpita, N. C. Structure and Biogenesis of the Cell Walls of Grasses. *Annu. Rev. Plant Physiol. Plant Mol. Biol.* **1996**, *47*, 445−476.
(25) Mourtzinis, S.; Cantrell, K. B.; Arriaga, F. J.; Balkcom, K. S.; Novak, J. M.; Frederick, J. R.; Karlen, D. L. Distribution of Structural Carbohydrates in Corn Plants Across the Southeastern USA. *Bioenerg. Res.* **2014**, *7*, 551−558.
(26) Burton, R. A.; Fincher, G. B. Current challenges in cell wall biology in the cereals and grasses. *Front. Plant Sci.* **2012**, *3*, 130.
(27) Park, Y. B.; Cosgrove, D. J. Xyloglucan and its Interactions with Other Components of the Growing Cell Wall. *Plant Cell Physiol.* **2015**, *56*, 180−194.
(28) Thomas, J. R.; Darvill, A. G.; Albersheim, P. Structure of Plant-Cell Walls .25. Rhamnogalacturonan-I, a Pectic Polysaccharide That Is a Component of Monocot Cell-Walls. *Carbohyd. Res.* **1989**, *185*, 279−305.
(29) Zykwinska, A.; Thibault, J.-F.; Ralet, M.-C. Organization of pectic arabinan and galactan side chains in association with cellulose microfibrils in primary cell walls and related models envisaged. *J. Exp. Bot.* **2007**, *58*, 1795−1802.
(30) Galloway, A. F.; Pedersen, M. J.; Merry, B.; Marcus, S. E.; Blacker, J.; Benning, L. G.; Field, K. J.; Knox, J. P. Xyloglucan is released by plants and promotes soil particle aggregation. *New Phytol.* **2018**, *217*, 1128−1136.
(31) Delannoy-Bruno, O.; Desai, C.; Raman, A. S.; Chen, R. Y.; Hibberd, M. C.; Cheng, J.; Han, N.; Castillo, J. J.; Couture, G.; Lebrilla, C. B.; Barve, R. A.; Lombard, V.; Henrissat, B.; Leyn, S. A.; Rodionov, D. A.; Osterman, A. L.; Hayashi, D. K.; Meynier, A.; Vinoy, S.; Kirbach, K.; Wilmot, T.; Heath, A. C.; Klein, S.; Barratt, M. J.; Gordon, J. I. Evaluating microbiome-directed fibre snacks in gnotobiotic mice and humans. *Nature* **2021**, *595*, 91−95.
(32) Zhang, Y.; Pribil, M.; Palmgren, M.; Gao, C. A CRISPR way for accelerating improvement of food crops. *Nat. Food* **2020**, *1*, 200−205.
(33) Zhang, Q.; Cheetamun, R.; Dhugga, K. S.; Rafalski, J. A.; Tingey, S. V.; Shirley, N. J.; Taylor, J.; Hayes, K.; Beatty, M.; Bacic, A.; Burton, R. A.; Fincher, G. B. Spatial gradients in cell wall composition and transcriptional profiles along elongating maize internodes. *BMC Plant Biol.* **2014**, *14*, 27.
(34) Arnaud, B.; Durand, S.; Fanuel, M.; Guillon, F.; Méchin, V.; Rogniaux, H. Imaging Study by Mass Spectrometry of the Spatial Variation of Cellulose and Hemicellulose Structures in Corn Stalks. *J. Agric. Food Chem.* **2020**, *68*, 4042−4050.
(35) Abedon, B. G.; Hatfield, R. D.; Tracy, W. F. Cell wall composition in juvenile and adult leaves of maize (Zea mays L.). *J. Agric. Food Chem.* **2006**, *54*, 3896−3900.
(36) Cosgrove, D. J. Growth of the plant cell wall. *Nat. Rev. Mol. Cell Biol.* **2005**, *6*, 850−861.
(37) Carpita, N. C.; McCann, M. C. The functions of cell wall polysaccharides in composition and architecture revealed through mutations. *Plant Soil* **2002**, *247*, 71−80.
(38) Costa, T. H. F.; Vega-Sanchez, M. E.; Milagres, A. M. F.; Scheller, H. V.; Ferraz, A. Tissue-specific distribution of hemicelluloses in six different sugarcane hybrids as related to cell wall recalcitrance. *Biotechnol. Biofuels* **2016**, *9*, 99.
(39) Faust, S.; Kaiser, K.; Wiedner, K.; Glaser, B.; Joergensen, R. G. Comparison of different methods for determining lignin concentration and quality in herbaceous and woody plant residues. *Plant Soil* **2018**, *433*, 7−18.
(40) Zhao, F.; Chen, W.; Sechet, J.; Martin, M.; Bovio, S.; Lionnet, C.; Long, Y.; Battu, V.; Mouille, G.; Monéger, F.; Traas, J. XyloglucansMicrotubules Synergistically Xyloglucans and Microtubules Synergistically Maintain Meristem Geometry and Phyllotaxis. *Plant Physiol.* **2019**, *181*, 1191−1206.
(41) Hsieh, Y. S. Y.; Harris, P. J. Xyloglucans of Monocotyledons Have Diverse Structures. *Mol. Plant* **2009**, *2*, 943−965.
(42) Hensel, A. Xyloglucane - Struktur, Genese und Funktionen einer weit verbreiteten Stoffgruppe. *Pharm. Unserer Zeit* **1993**, *22*, 228−234.
(43) Kozlova, L. V.; Nazipova, A. R.; Gorshkov, O. V.; Petrova, A. A.; Gorshkova, T. A. Elongating maize root: zone-specific combinations of polysaccharides from type I and type II primary cell walls. *Sci. Rep.* **2020**, *10*, 10956.
(44) Roulin, S.; Feller, U. Reversible accumulation of (1→3,1→4)-*β*-glucan endohydrolase in wheat leaves under sugar depletion. *J. Exp. Bot.* **2001**, *52*, 2323−2332.
(45) Roulin, S.; Buchala, A.; Fincher, G. Induction of (1→3,1→4)-*- D -glucan hydrolases in leaves of dark-incubated barley seedlings. *Planta* **2002**, *215*, 51−59.
(46) Vega-Sanchez, M.; Verhertbruggen, Y.; Scheller, H. V.; Ronald, P. Abundance of mixed linkage glucan in mature tissues and secondary cell walls of grasses. *Plant Signal Behav.* **2013**, *8*, No. e23143.
(47) Willats, W. G. T.; McCartney, L.; Mackie, W.; Knox, J. P. Pectin: cell biology and prospects for functional analysis. *Plant Mol. Biol.* **2001**, *47*, 9−27.

https://doi.org/10.1021/acsfoodscitech.1c00318
ACS Food Sci. Technol. 2021, 1, 2117−2126